

The Dynamics of Bunched Laser-Cooled Ion Beams at Relativistic Energies

M Bussmann¹, U Schramm², D Habs¹, M Steck³, T Kühl³, K Beckert³, P Beller³, B Franzke³, W Nörtershäuser^{3,6}, C Geppert^{3,6}, C Novotny^{3,6}, J Kluge³, F Nolden³, T Stöhlker³, C Kozhuharov³, S Reinhardt⁴, G Saathoff⁵, S Karpuk⁶

¹ Ludwig-Maximilians Universität München, Am Coulombwall 1, D-85748 Garching, Germany

² Forschungszentrum Dresden-Rossendorf e.V., Bautzner Landstrasse 128, D-01328 Dresden, Germany

³ Gesellschaft für Schwerionenforschung mbH, Planckstrasse 1, D-64291 Darmstadt, Germany

⁴ Max-Planck-Institut für Kernphysik, Saupfercheckweg 1, D-69117 Heidelberg, Germany

⁵ Max-Planck-Institut für Quantenoptik, Hans-Kopfermann-Strasse 1, D-85748 Garching, Germany

⁶ Johannes-Gutenberg Universität Mainz, Staudingerweg 7, D-55128 Mainz, Germany

E-mail: michael.bussmann@physik.uni-muenchen.de

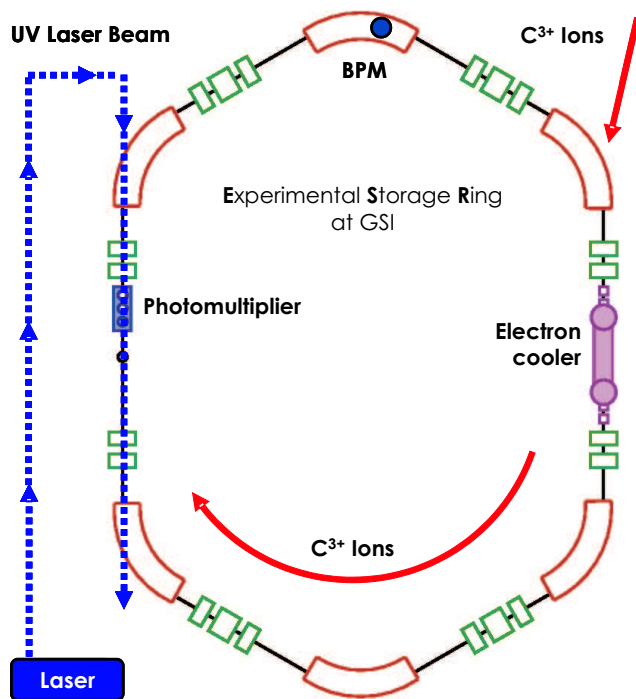
Abstract. We discuss the axial dynamics of laser-cooled relativistic C³⁺ ion beams at moderate bunching voltages. Schottky noise spectra measured at a beam energy of 122 MeV/u are compared to simulations of the axial beam dynamics. Ions confined in the bucket are addressed by the narrow-band force of a laser beam counter-propagating to the ion beam, while the laser frequency is detuned relatively to the cooling transition frequency in the rest frame of the bucket.

At large detuning comparable to the momentum acceptance of the bucket, the axial dynamics can be well explained by the secular motion of individual non-interacting ions. At small detuning, corresponding to a small axial momentum spread $\Delta p_{\text{axial}}/p_{\text{axial}} < 10^{-6}$ of the ions, the measured Schottky noise spectra can no longer be explained using an approach which neglects the ion-ion interaction. Instead, the model fails when the ion bunch enters the *space-charge dominated* regime, at which the mutual Coulomb-energy of the ions becomes comparable to the kinetic energy of the ions.

1. Introduction

Laser-cooling of bunched ion beams, as first demonstrated in the *ASTRID* storage ring [1], utilises the restoring force of the bucket to counteract the laser force. This cooling scheme does not require a laser beam co-propagating with the ion beam. Instead, only one laser beam counter-propagating to the ion beam is needed to provide a momentum-dependent friction force which damps the synchrotron oscillation of the ions in the bucket. While the ions oscillate in the bucket, those ions in resonance with the laser light are cooled by the combined forces of the bucket and the laser.

Before laser-cooling is applied, the momentum distribution of the bucket resembles the momentum acceptance of the bucket, which is approximately $\Delta p_{\text{acc,b}}/p_{\text{acc,b}} \approx 2 \times 10^{-5}$ in the experiment discussed here. The momentum acceptance of the laser force of about



ESR Parameters	
Circumference	108,36 m
Betatron tune	2.3
Slip factor	0.607
<hr/>	
Ion Species	C ³⁺
Beam Energy	1.47 GeV
relativistic β, γ	0.47, 1.13
revolution frequency	1.295 MHz
lifetime	450 s
<hr/>	
Laser Parameters	
Laser Source	Ar ⁺ ion laser
Operational Mode	cw, single mode, single frequency
Wave Length	257.34 nm (SHG)
Power	40-100 mW
<hr/>	
Cooling Transitions [2]	
2S _{1/2} → 2P _{1/2}	155.07 nm
2S _{1/2} → 2P _{3/2}	155.81 nm

Figure 1. *Left:* (color online) Schematic view of the *Experimental Storage Ring* ESR at GSI in Darmstadt. The C³⁺ ions circulate clockwise in the ring. The ion beam is overlapped with the counter-propagating laser beam in a straight section of the ring. The laser beam focus is placed at the position of the photomultiplier to maximize the fluorescence light intensity. *Right:* List of experimental parameters.

$\Delta p_{acc,1}/p_{acc,1} \approx 5 \times 10^{-8}$ does not match the initial momentum distribution of the hot ions. Two cooling schemes exist to overcome this mismatch, which both rely on detuning the laser frequency relative to the frequency of the cooling transition for ions at rest in the bucket center. This can be done either by scanning the laser frequency directly or by changing the bunching frequency and keeping the laser frequency fixed. The latter scheme provides a wider detuning range as is accessible with the laser system which was used in the experiment and will thus be the focus of this work. In the following, the experimental conditions will be briefly summarized, before the dynamics of the ions in the bucket and the corresponding beam characteristics will be discussed in detail.

2. Experimental Setup

Laser-cooling is provided using a continuous-wave, single mode, single frequency argon ion laser system. After doubling the laser frequency to $\lambda_{l,lab}/2 = 257.34$ nm, the laser beam is overlapped with the C³⁺ ion beam – see Fig. 1 for a schematic overview of the storage ring including a list of the most important experimental parameters. With the ion beam energy set to 1.47 GeV, the relativistic Doppler shift of the laser wave length from the laboratory frame to the ion rest frame [3] amounts to

$$\lambda_{l,rest} = \frac{\lambda_{l,lab}/2}{\gamma(1 + \beta)} \approx \frac{257.34 \text{ nm}}{1.13 \times (1 + 0.47)} \approx 155 \text{ nm}, \quad (1)$$

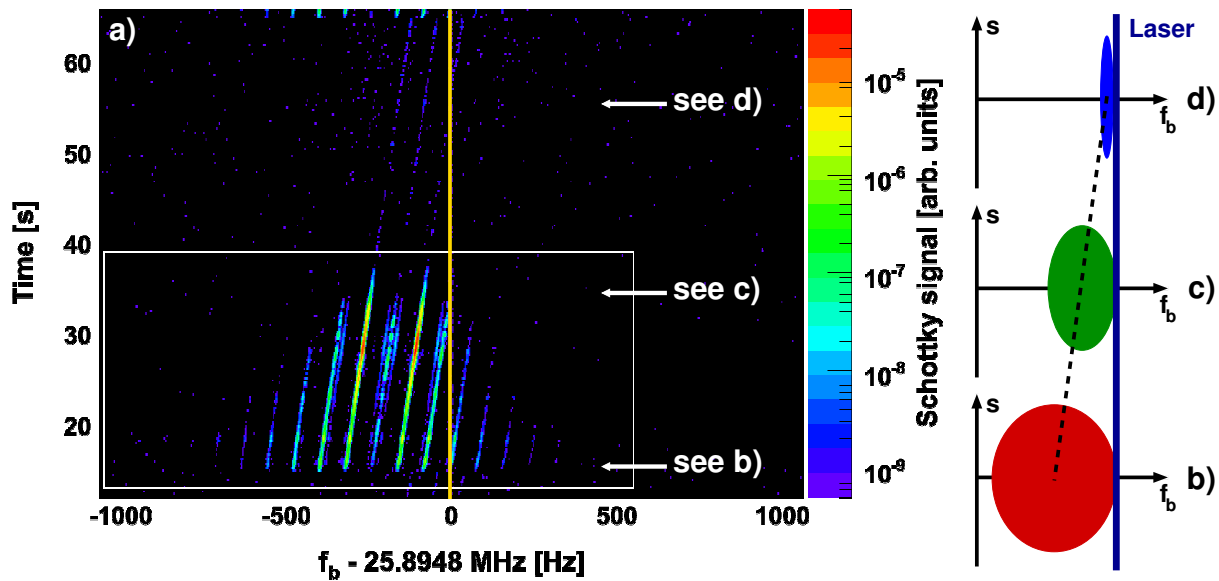


Figure 2. (color online) *a)* Schottky noise signal versus scanning time. The intensity is colour-coded. The white box encloses the part of the spectrum discussed in Fig. 3. The yellow line marks the (fixed) position of the laser frequency relative to the bunching frequency.

b)–d) Schematic view of the ion bunch (ellipse) at three distinct values of the absolute detuning. The absolute detuning of the bunching frequency relative to the laser frequency decreases from Fig. b) to d) as indicated by the black dotted line. The position of the laser is marked by the solid blue line.

b) The laser is close to the separatrix. A number of sidebands can be seen which indicate the momentum spread of the beam.

c) The absolute detuning has been reduced, the ion bunch is now space-charge dominated.

d) The absolute detuning has almost reached its minimum value. No blowup of the beam due to intra beam scattering is observed.

assuming the orientation of the ion beam and the laser beam to be anti-parallel.

Compared to bunched beams typically provided in storage rings, the moderate bunching voltages of only a few volts resulted in weak axial confinement of the ions and thus in bunch lengths of about 1 m at ion currents on the order of 10 μ A. Measurements of the beam parameters were performed for various bunching frequencies $f_b = h \times f_{\text{rev}}$ subsequently set to the 5th, 10th and 20th harmonic h of the revolution frequency f_{rev} . Given a betatron tune of $Q = 2.3$ [4], the betatron frequency $f_{\text{beta}} = Q \times f_{\text{rev}} \approx 2.9785$ MHz is orders of magnitude larger than the synchrotron frequency of $f_{\text{sync}} \approx 188$ Hz measured for the 20th harmonic at a bunching voltage of about $U_b \approx 7$ V. The bunch form thus resembles an ellipsoid elongated in the axial direction.

3. Detuning the bunching frequency relatively to the laser frequency

In the following we focus on a single series of Schottky signals recorded at a bunching frequency of $f_{b,0} \approx 20 \times f_{\text{rev}} \approx 25.894750$ MHz, previously discussed in [5]. The sign of the bunching frequency detuning $\Delta f_b = f_b - f_{b,0}$ indicates whether the bucket force and the laser force are opposed to each other (negative Δf_b), thus providing a net cooling force, or if both point in the same direction (positive sign). When both the bucket force and the laser force point in the same direction, the ions are driven out of the bucket by the combined bunching and laser force. The change from negative to positive detuning Δf_b thus easily marks the bunching frequency

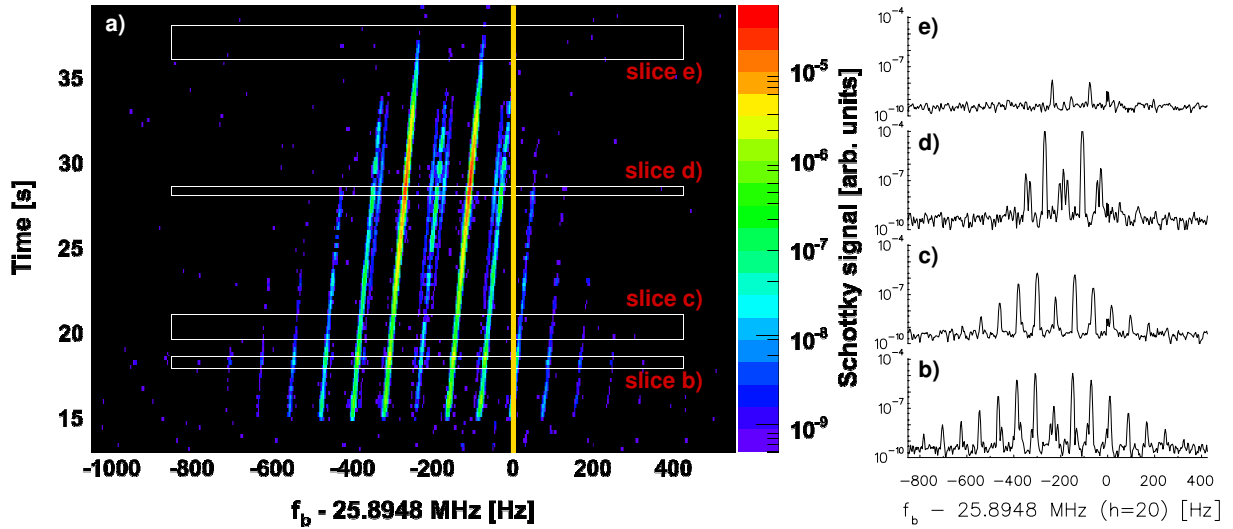


Figure 3. (color online) *a)* Schottky noise signal versus scanning time. This is a detailed view of the region marked by the white box in Fig. 2. The intensity is colour-coded. The white boxes indicate the slices shown in Part *b)*–*e)* of this figure. Again, the yellow line marks the (fixed) position of the laser frequency relative to the bunching frequency. *b)*–*e)* Slices selected from the time evolution of the Schottky signal. The absolute detuning of the bunching frequency relative to the laser frequency decreases from Fig. *b)* to *e)*. The amplitudes of the curves are normalized with respect to the time for which the slice is integrated.

$f_{b,0}$ at which those ions at rest in the bucket are in resonance with the laser frequency. The bunching frequency is detuned at a rate of 10 Hz per second, meaning that every second the bunching frequency is increased by 10 Hz in a single step. During the scan the laser frequency is kept at a fixed value. The scan of the bucket frequency starts with the laser frequency being near the brim of the separatrix, meaning that the relative detuning of the bucket frequency is of the same order as the relative momentum acceptance

$$\frac{\Delta p_{acc,b}}{p_{acc,b}} \approx 2 \times 10^{-5} \approx \frac{1}{\eta} \frac{|\Delta f_b|}{f_b} \quad (2)$$

of the bucket. Both are related by the slip factor η [4]. When the absolute detuning is reduced, subsequently ions with lower relative momentum come in resonance with the laser force and are thus cooled. The total axial momentum spread is therefore reduced during the scan of the bucket frequency. This cooling scheme relies on the cooling time being much faster than the time for the frequency scan (for an estimate of the cooling time see [3]). Furthermore, intra-beam scattering (IBS) can cause fast heating of the ions, which can lead to a sudden increase of the axial momentum that cannot be counteracted by a single, narrow-band laser. A schematic view of the cooling scheme is shown in Fig. 2. The total axial momentum spread of the beam is determined by the position of the laser frequency in momentum space, so that

$$\frac{\Delta p_{axial}}{p_{axial}} \lesssim \frac{1}{\eta} \frac{|\Delta f_b|}{f_b}, \quad (3)$$

as long as no strong heating due to IBS occurs.

4. A detailed discussion of Schottky noise spectra

Fig. 3 *a)* shows a colour-coded plot of the Schottky noise spectrum. The intensity of the Schottky signal is scaled logarithmically, the Y-axis shows the scanning time and the X-axis

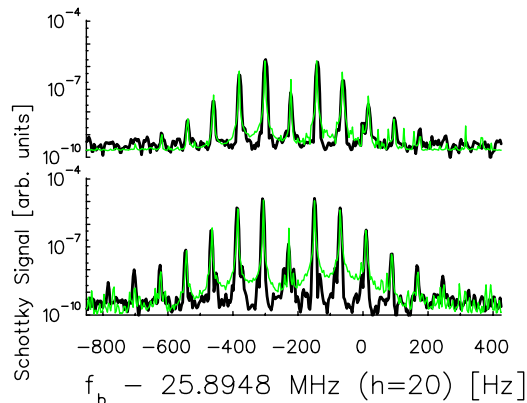


Figure 4. (color online) Slices taken from the Schottky noise spectrum as shown in Fig. 3 b) (lower part) and c) (upper part).

The black curves show the measured data while the green curves depict the simulation result. Spacing, total position and relative intensity of the carrier to the sidebands are well matched by the simulation. The increased pedestal can be attributed to the number of ions used in the simulation, which was about a factor 1000 smaller than in the measurement. The simulation data was scaled in intensity to match the measured curves.

the bunch frequency. The yellow line illustrates the fixed position of the laser frequency. Four slices marked b), c), d) and e) are selected from the time evolution of the Schottky spectrum as indicated by four white boxes.

With decreasing absolute detuning the momentum spread, corresponding to the number of side bands visible in the spectrum, decreases. In Fig. 3 b) the laser frequency is located near the brim of the separatrix, while in part c) the momentum spread is already significantly reduced. Part d) of Fig. 3 marks the transition from an axially emittance dominated beam to a space-charge dominated [6] beam. A detailed analysis of this transition is given in [5], indicating that the linear density of the bunch remains constant for smaller absolute detuning [7], while the axial momentum spread of the beam becomes smaller than the resolution of the Schottky pickup measurement. Finally, part e) of Fig. 3 shows a Schottky spectrum at small absolute detuning. In the following we will focus on two features of the time evolution of the spectra. First, the reduced intensity of the carrier signal compared to the intensity of the side bands. Second, the overall reduction of the intensity of the Schottky noise signal, which finally leads to an almost vanishing signal at small absolute detuning.

5. Axial dynamics of the laser-cooled ions in the bucket

In a simple, yet far reaching simulation of the axial dynamics of the laser-cooled ions in the bucket, we assume that the ions do not interact with each other, but instead can oscillate independently in a harmonic bucket potential. The detuning of the laser force is set according to the measured spectra shown in Fig. 3 b) and c). The axial momentum spread of the ions is precisely reproduced by setting $\Delta p_{\text{axial}}/p_{\text{axial}} \equiv |\Delta f_b|/(\eta f_b)$.

The reduction of the carrier intensity can be simulated by a collective axial oscillation of the ions in the bunch. The amplitude of this oscillation is bounded by the position of the laser force in the bucket well, meaning that the amplitude can be derived by equating the maximum potential energy of the ions with the energy difference given by the absolute detuning of the laser frequency relative to the bucket center.

The collective oscillation itself can be understood by looking closer at the experimental realization of the cooling scheme. Instead of continuously changing the bunching frequency, it has been changed stepwise, thus altering the position of the bucket in momentum space abruptly. We attribute the collective oscillation of the ions in the bucket to this abrupt change in the position of the bucket minimum. The only force counteracting the oscillation is the laser force, which rapidly damps all oscillation amplitudes exceeding the barrier defined by the position of the laser frequency relative to the bucket center.

Thus, assuming both the amplitude of the collective oscillation and the momentum spread of the ions are bounded by the absolute detuning, the Schottky noise spectra depicted in Fig. 3 b)

and c) are reproduced by the simulation, as can be seen in Fig. 4.

Besides the physical characteristics of the Schottky spectra, numerical artefacts due to the underlying Fast-Fourier-Transformation (FFT) algorithm are found both in simulation and experimental data. Namely, the amplitude of the satellite side bands, which appear in 3 d) next to the two regular first order side bands, could be both increased and decreased to zero depending on the number of revolutions of the beam used as an input for the FFT. They could thus be identified to have no physical significance.

6. Schottky noise spectra of space-charge dominated beams

This situation changes when $|\Delta f_b|$ is further reduced. While in the simulation the carrier signal increases drastically, the measurement shows an almost vanishing carrier signal and a further reduction of the first side bands.

In the simulation, the increase of the carrier signal is caused by the reduction of the collective oscillation amplitude. The simulated Schottky noise signal therefore becomes equal to the signal of a stationary ensemble of non-interacting ions resting in the bucket, for which the intensity of the carrier signal is proportional to the number of particles confined in the bucket [8].

The simulation can no longer be brought in accordance with the experimental data when the beam becomes space-charge dominated in the axial direction. In particular, it does not reproduce the decreasing signal strength of the Schottky signal. In the emittance-dominated regime, which is well described by the simulation, the ion dynamics can be modeled neglecting the Coulomb interaction of the ions, since the kinetic energy of the ions is much larger than the mutual Coulomb energy. However, in the space-charge dominated regime, the kinetic energy of the ions is reduced to values where it becomes comparable to the mutual Coulomb energy [6]. The simulation model therefore has to fail.

7. Conclusion and Outlook

We have shown that a simple model of non-interacting, laser-cooled ions confined in a bucket can reproduce the Schottky noise spectra of emittance-dominated bunched ion beams. At the transition from the emittance-dominated regime to the space-charge dominated regime, the model fails. Currently, no convincing explanation for the observed evolution of the spectra in the space-charge dominated regime exists.

We are currently modifying the experimental setup to overcome the diagnostic limitation of the Schottky measurement and extend the precision of the momentum spread determination based on measuring the fluorescence intensity of the ions in the direct vicinity of the beam. These experimental modifications will be accompanied by a complete, realistic simulation of the ion dynamics in the bucket, which includes the Coulomb-interaction of the ions.

This work was supported by the German BMBF (06ML183).

References

- [1] Hangst J S, Nielsen J S, Poulsen O, Shi P and Schiffer J P 1995 *Phys. Rev. Lett.* **74** 4432–4435
- [2] Schramm U, Bussmann M, Habs D, Steck M, Kühl T, Beckert K, Beller P, Franzke B, Nolden F, Saathoff G, Reinhardt S and Karpuk S 2005 *Hyperfine Interactions* **162** 181–188
- [3] Schramm U, Bussmann M and Habs D 2004 *Nuclear Instruments and Methods in Physics Research Section A: Accelerators, Spectrometers, Detectors and Associated Equipment* **532** 348–356
- [4] Schramm U and Habs D 2004 *Progress in Particle and Nuclear Physics* **53** 583–677
- [5] Schramm U, Bussmann M, Habs D, Steck M, Kühl T, Beckert K, Beller P, Franzke B, Nolden F, Saathoff G, Reinhardt S and Karpuk S 2005 *Proceedings of the 2005 Particle Accelerator Conference, PAC05* 401–403
- [6] Dubin D H E and O’Neil T M 1999 *Rev. Mod. Phys.* **71** 87
- [7] Ellison T J P, Nagaitsev S S, Ball M S, Caussyn D D, Ellison M J and Hamilton B J 1993 *Phys. Rev. Lett.* **70** 790–793
- [8] Boussard D 1987 *CERN Accelerator School* **87-03** 416–452